Appendix 1 - Full description of the search strategies

1.1. Cochrane Library

The search was done in "Search Manager" in "Advanced Search".

The used search terms were:

((electroporation OR electropermeabilization OR nanoknife) AND ("in silico" OR mathemat* OR numeric* OR parametric* OR simulation OR theoretic* OR theory OR computation* OR "finite element" OR "finite difference" OR thermal OR temperature)):ti,ab,kw

1.2. Embase

The search was done in "Basic Search". In section "Limits" the check boxes were not checked off.

The used search terms were:

((electroporation OR electropermeabilization OR nanoknife) AND ("in silico" OR mathemat$ OR numeric$ OR parametric$ OR simulation OR theoretic$ OR theory OR computation$ OR "finite element" OR "finite difference" OR thermal OR temperature)).ti,ab,kw.

1.3. IEEE Xplore Digital Library

The search was done in "Command Search" in "Advanced Search". Here, the check circle of "Metadata Only" was checked off. The used search terms were:

(((electroporation OR electropermeabilization OR nanoknife) AND ("in silico" OR mathemat* OR numeric* OR parametric* OR simulation OR theoretic* OR theory OR computation* OR "finite element" OR "finite difference" OR thermal OR temperature)))

1.4. PubMed

The search was done in "Basic Search". The used search terms were:

((electroporation[Text word] OR electropermeabilization[Text word] OR nanoknife[Text word]) AND ("in silico"[Text word] OR mathemat*[Text word] OR numeric*[Text word] OR parametric*[Text word] OR simulation[Text word] OR theoretic*[Text word] OR theory[Text word] OR computation*[Text word] OR "finite element"[Text word] OR "finite difference"[Text word] OR thermal[Text word] OR temperature[Text word]))

1.5. Science Direct

The search was done in "Title, abstract or keywords" in "Advanced search". The check boxes in "Show more fields" were not checked off. The used search terms were:

((electroporation OR electropermeabilization OR nanoknife) AND ("in silico" OR mathemat OR numeric OR parametric OR simulation OR theoretic OR theory OR computation OR "finite element" OR "finite difference" OR thermal OR temperature))

1.6. Scopus

The search was done in the tab "Advanced" in "Search". The used search terms were:

TITLE-ABS-KEY(((electroporation OR electropermeabilization OR nanoknife) AND ("in silico" OR mathemat* OR numeric* OR parametric* OR simulation OR theoretic* OR theory OR computation* OR "finite element" OR "finite difference" OR thermal OR temperature)))

1.7. Web of Science

The search was done in "Advanced search". The following check boxes, and circles were checked off:

- All languages
- All document types
- All Years
- More Settings
- Science Citation Index Expanded (SCI-EXPANDED) --1975-present
- Social Sciences Citation Index (SSCI) --1975-present
- Arts & Humanities Citation Index (A&HCI) --1975-present
- Emerging Sources Citation Index (ESCI) --2015-present

The used search terms were:

TS=(((electroporation OR electropermeabilization OR nanoknife) AND ("in silico" OR mathemat* OR numeric* OR parametric* OR simulation OR theoretic* OR theory OR computation* OR "finite element" OR "finite difference" OR thermal OR temperature)))

Appendix 2 - Definitions of abbreviations, symbols and extracted parameters

Table A2.1

Table A2.1 Definitions of the used symbols.

Abbreviations and symbols of quantities	Unit [symbol]	Definition
BC		Boundary condition.
BEM		Boundaries between the electrodes and the media.
BOS		Boundaries at the outer surface of the model.
CAR		Cardiac autosynchronous rate.
CEM43°C	[min]	Cumulative equivalent minutes at 43 °C.
CEM43°C$_{(th)}$	[min]	Threshold of cumulative equivalent minutes at 43 °C that can results in thermal damage.
IPE		Irreversible permeabilization effect (we chose IPE instead of IRE effect to distinguish between only the permeabilization effect, and the permeabilization and the thermal effects jointly produced by IRE).
IRE		Irreversible electroporation.
IRE-TR		Region treated by IRE.
MH		Mild hyperthermia.
MWA		Microwave ablation.
NA		Not applicable.
NC		Not clear.
ND		Not defined.
NR		Data is not reported in the included study.
NTA		No thermal analysis.
RE		Reversible electroporation.
RFA		Radiofrequency ablation.
TA		Thermal ablation.
$\boldsymbol{n}$	[m]	Normal vector that is perpendicular to any surface in a model.
$\boldsymbol{E}$	[V·m^{-1}]	Electric-field vector.
$\boldsymbol{J}$	[A·m^{-2}]	Electric-current density.
$\boldsymbol{J_e}$	[A·m^{-2}]	Externally generated electric-current density.
$\boldsymbol{J} \cdot \boldsymbol{E}$	[W·m^{-3}]	The Joule Heating term; the heat generation rate per unit volume.
$\boldsymbol{H}$	[A·m^{-1}]	Magnetic-field vector.
∇	[m^{-1}]	Gradient.
$\nabla \cdot$	[m^{-1}]	Divergence.
$\nabla \times$	[m^{-1}]	Curl.
∇^2	[m^{-2}]	Laplace operator.
$\underline{\nabla}$		Dimensionless gradient.
$\underline{\nabla} \cdot$		Dimensionless divergence.
$\underline{\nabla}^2$		Dimensionless Laplace operator.
i#, j#, k#, l#, m#, n#		Iteration numbers.

Abbreviations and symbols of quantities	Unit [symbol]	Definition
a	$[W \cdot m^{-2} \cdot °C^{-4}]$	Stefan-Boltzmann constant.
$a_{n\#}$		Parameters of sigmoid function.
c_b	$[J \cdot kg^{-1} \cdot °C^{-1}]$	Specific heat capacity of blood.
c_p	$[J \cdot kg^{-1} \cdot °C^{-1}]$	Specific heat capacity of a medium.
d	$[m]$	Center-to-center distance between the electrodes in case of cylindrical or spherical electrodes; the distance between the electrodes in case of plate electrodes.
dt	$[s]$ or $[min]$	Time differential.
f_P	$[Hz]$	Pulse frequency.
h	$[W \cdot m^{-2} \cdot °C^{-1}]$	Heat transfer coefficient.
h_{eq}	$[W \cdot m^{-2} \cdot °C^{-1}]$	Equivalent heat transfer coefficient.
j		$j = (-1)^{0.5}$.
k	$[W \cdot m^{-1} \cdot °C^{-1}]$	Constant thermal conductivity of a medium.
k_{init}	$[W \cdot m^{-1} \cdot °C^{-1}]$	Initial thermal conductivity of a medium before the start of a heating process.
min		Minimum value.
max		Maximal value.
n	$[m]$	Magnitude of the normal vector.
n_P		Pulse number.
q	$[C \cdot m^{-3}]$	Charge density.
q_e	$[W \cdot m^{-2}]$	Evaporation rate.
q_{BEM}	$[W \cdot m^{-2}]$	Heat flux through boundaries between electrode and media.
q_{BOS}	$[W \cdot m^{-2}]$	Heat flux through the outer surface of the model.
r	$[m]$	Radial coordinate.
r_{fit}	$[m]$	Variable fitted to 1D temperature distribution.
t	$[s]$	Time.
$\underline{t}$		Dimensionless time.
t_{init}	$[s]$	Start time of a heating process.
t_{43}	$[min]$	Thermal isoeffect dose.
t_{end}	$[s]$	Ending time of a heating process.
t_{MH}	$[s]$	Start time of mild hyperthermia.
t_{TA}	$[s]$	Start time of thermal ablation.
t_P	$[s]$	Single pulse duration.
u	$[J \cdot m^{-3}]$	Energy density.
w_b	$[kg \cdot m^{-3} \cdot s^{-1}]$	Blood perfusion.
x	$[m]$	The Cartesian coordinate.
$\underline{x}$		Dimensionless Cartesian coordinate.
y	$[m]$	The Cartesian coordinate.
$\underline{y}$		Dimensionless Cartesian coordinate.
z	$[m]$	The Cartesian coordinate.
$\underline{z}$		Dimensionless Cartesian coordinate.
A	$[s^{-1}]$	Pre-exponential factor (Collision frequency).

Abbreviations and symbols of quantities	Unit [symbol]	Definition
D	[m]	Distance between the electrodes in case of cylindrical or spherical electrodes, excluding the electrode diameter; the distance between the electrodes in case of plate electrodes.
$E = \|\boldsymbol{E}\|$	[V·m^{-1}]	Magnitude of an electric-field vector.
E_{alt}	[V·m^{-1}]	Electric-field magnitude at which the electrical conductivity starts to change.
E_{range}	[V·m^{-1}]	Electric-field magnitude range at which the electrical conductivity changes.
$E_{RE(th)}$	[V·m^{-1}]	Electric-field threshold of reversible electroporation; minimum electric-field value that reversibly permeabilizes specific cells/tissue during RE.
$E_{IRE(th)}$	[V·m^{-1}]	Electric-field threshold of irreversible electroporation; minimum electric-field value that ablates target cells/tissue during IRE. Even though $E_{IRE(th)}$ was only used as a minimum required E to extract $S_{E\text{-}IRE(th),\Sigma}$ for this analysis, it must be noticed that $E_{IRE(th)}$ in reality also depends on pulse parameters (pulse voltage, pulse shape, pulse length, pulse number and pulse frequency, temperature and electrical conductivity of the target.
I#, J#, K#, L#, M#, N#		Total iteration number.
I_{BOS}	[A]	Electric current through outer surface of the model.
L	[m]	Active length.
$N(t_{init})$		Number of intact substances in the tissue before the treatment.
$N(t)$		Number of intact substances in the tissue at time point t.
N_P		Total number of pulses.
$\underline{P}$		Dimensionless Joule-Heating term.
Q_m	[W·m^{-3}]	Metabolic heat generation.
V_P	[V]	Electric potential of the pulses.
$\dot{R}$	[J·mol^{-1}·K^{-1}]	Ideal gas constant.
R		Factor to compensate for a 1 °C temperature change.
$R_{3\Delta T13}$	[%]	Ratio between the sizes of the region with mild-hyperthermic temperature increase and irreversibly permeabilized region.
$R_{\Delta T13}$	[%]	The ratio between the sizes of thermally ablated region and irreversibly permeabilized region.

Abbreviations and symbols of quantities	Unit [symbol]	Definition
$R\Delta t_{MH}$		Dimensionless ratio between the time duration of mild hyperthermia and total treatment time.
$R\Delta t_{TA}$		Dimensionless ratio between the time duration of thermal ablation and total treatment time.
$S_{\Delta T}$	$[m^2]$	The surface area of the simulated temperature increase in a 2D plot.
$S_{3\Delta T13}$	$[m^2]$	The surface area of the simulated temperature increase in a 2D plot within the range $3 \leq \Delta T$ [°C] < 13 excluding the surface area of the electrodes.
$S_{3\Delta T13,\Sigma}$	$[m^2]$	The total surface area of the simulated temperature increase in a 2D plot within the range $3 \leq \Delta T$ [°C] < 13 excluding the surface area of the electrodes.
$S_{\Delta T13}$	$[m^2]$	The surface area of the simulated temperature increase in a 2D plot that is at least 13 °C excluding the surface area of the electrodes.
$S_{\Delta T13,\Sigma}$	$[m^2]$	The total surface area of the simulated temperature increase in a 2D plot that is at least 13 °C excluding the surface area of the electrodes.
S_E	$[m^2]$	The surface area of the electric field in a 2D plot with an electric-field magnitude at least $E_{IRE(th)}$ including the surface area of the electrodes.
$S_{E-IRE(th)}$	$[m^2]$	The surface area of the electric field in a 2D plot with an electric-field magnitude at least $E_{IRE(th)}$ excluding the surface area of the electrodes.
$S_{E-IRE(th),\Sigma}$	$[m^2]$	The total surface area of the electric field in a 2D plot with an electric-field magnitude at least $E_{IRE(th)}$ excluding the surface area of the electrodes.
S_{elect}	$[m^2]$	The surface area of the electrode in a single IRE-TR in a 2D plot.
$S_{elect,\Sigma}$	$[m^2]$	The total surface area of the electrodes in a single IRE-TR in a 2D plot.
T	[°C]	Temperature.
$\underline{T}$		Dimensionless temperature.
T_{art}	[°C]	Arterial blood temperature.
T_{BEM}	[°C]	Temperature value at the boundaries between the electrode and the media.
T_{BOS}	[°C]	Temperature value at the outer surface of the model.
T_{dt}	[°C]	The average temperature over the period dt.
T_{env}	[°C]	Temperature of the environment.
T_{fit}	[°C]	Variable fitted to 1D temperature distribution.

Abbreviations and symbols of quantities	Unit [symbol]	Definition
T_{init}	[°C]	Initial physiological temperature.
T_{min}	[°C]	Minimum obtained temperature.
T_{max}	[°C]	Maximum obtained temperature.
$T_K(t)$	[K]	Time dependent absolute temperature.
T_{th}	[°C]	Thermally ablative threshold.
X	[°C]	Temporarily variable.
U_a	[J·mol^{-1}]	Activation energy.
V_P	[V]	Scalar electric potential (voltage) of the pulses.
α	[m^2·s^{-1}]	Thermal diffusivity.
β_1		First constants of the Fourier Series.
$\beta_{n\#}$		Constants of the Fourier Series.
ε	[F·m^{-1}]	Permittivity of a medium.
ε_0	[F·m^{-1}]	Permittivity of free space.
ε_r		Relative permittivity.
ε_s		Emissivity of a surface area.
μ	[H·m^{-1}]	Permeability of a medium.
μ_0	[H·m^{-1}]	Permeability of free space.
μ_r		Relative Permeability.
ξ	[°C^{-1}]	Increase of (electrical or thermal) conductivity per 1 °C.
ρ	[kg·m^{-3}]	Mass density of a medium.
ρ_b	[kg·m^{-3}]	Blood density.
σ	[S·m^{-1}]	Constant electrical conductivity of a medium.
$\underline{\sigma}$		Normalized electrical conductivity.
σ_{init}	[S·m^{-1}]	Initial electrical conductivity; conductivity value before application of reversible or irreversible electroporation.
σ_{max}	[S·m^{-1}]	Maximum electrical conductivity that can be obtained during or after irreversible electroporation.
σ_t	[S·m^{-1}]	Electrical conductivity of a target volume.
$\sigma(n_P)$	[S·m^{-1}]	Electrical conductivity that depends on pulse number.
$\sigma(E)$	[S·m^{-1}]	Electrical conductivity that depends on electric-field magnitude.
$\sigma(T)$	[S·m^{-1}]	Electrical conductivity that depends on temperature.
$\sigma(E, T)$	[S·m^{-1}]	Electrical conductivity that depends on both electric-field magnitude and temperature.
τ	[s]	The time constant for heat conduction.
τ_P	[s]	Duration between two pulses.
ω	[rad·s^{-1}]	Angular frequency.
ω_b	[s^{-1} = mL·mL^{-1}·s^{-1}]	Blood perfusion rate.
Γ	[m]	Half thickness.
Δ		Difference.

Abbreviations and symbols of quantities	Unit [symbol]	Definition
Δt	[s]	Time duration.
Δt_{MH}	[s]	Time duration of mild-hyperthermic temperatures.
Δt_{TA}	[s]	Time duration of thermally ablative temperatures.
ΔT	[°C]	Temperature increase.
ΔT_{max}	[°C]	Maximum temperature increase.
ΔT_{MH}	[°C]	Maximal temperature increase during mild hyperthermia.
ΔT_{TA}	[°C]	Maximal temperature increase during thermal ablation.
Λ		Electroporation factor which considers the tissue permeabilization.
$\Omega(t)$		Time dependent accumulated thermal damage.
Ω_{th}		Accumulated thermal damage threshold.
Φ	[V]	Scalar electric potential.
$\underline{\Phi}$		Normalized scalar electric potential.
Φ_{BEM}	[V]	Scalar electric potential of the boundary condition at the medium electrode interface.
$\underline{\Phi}_{BEM}$		Normalized scalar electric potential of the boundary condition at the medium electrode interface.
Φ_{BOS}	[V]	Scalar electric potential of the boundary condition at the outer surface of the model.
$\underline{\Phi}_{BOS}$		Normalized scalar electric potential of the boundary condition at the outer surface of the model.
Υ	[%]	Probability of the thermal damage.
$\emptyset$	[m]	Diameter of an electrode with a cylinder shape.
$\mathbb{R}$		Set of real numbers.

Table A2.2

Table A2.2 Definitions of the extracted study characteristics.

Category	Study Charac-teristic	Definition
Medium properties	Compo-sition	The properties of the used mediums (organ/tissue) could be: • Homogeneous: The volume is composed of the same tissue type. • Heterogeneous: The volume is composed of at least two different tissue types. • Isotropic: The value of the property of the tissue is identical in all directions. • Anisotropic: The value of the property of the tissue is directionally depended. • Linear: The value of the property of the tissue is a constant. • Non-linear: The value of the property of the tissue depends on the electric-field strength, the number of pulses, the temperature and/or time.
Simulation results of the electric-field strength of irreversible electro-poration	Position of $S_{E\text{-}IRE(th)}$	Position of $S_{E\text{-}IRE(th)}$ in a figure provided by an included study with respect to the center of the figure.
	Number of $S_{E\text{-}IRE(th)}$	Number of electric-field areas with the condition $E \geq E_{IRE(th)}$ in the provided figure.
Simulation results of mild-hyperthermic effect where $03 \leq \Delta T \, [°C] < 13$	Position of $S_{3\Delta T13}$	Position of $S_{3\Delta T13}$ in a figure provided by an included study with respect to the center of the figure.
	Number of $S_{3\Delta T13}$	Number of temperature areas with the condition $3 \, °C \leq \Delta T < 13 \, °C$ in $S_{E\text{-}IRE(th)}$.
Simulation results of thermally ablative effect where $\Delta T \geq 13 \, °C$	Position of $S_{\Delta T13}$	Position of $S_{\Delta T13}$ in a figure provided by an included study with respect to the center of the figure.

	Number of $S_{\Delta T13}$	Number of temperature areas with the condition $\Delta T \geq 13\ °C$ in $S_{E\text{-}IRE(th)}$.

Appendix 3 - Extended mathematical description of IRE

For convenience, overviews of the symbols and the mathematical notations were summarized in Appendix 2.

3.1. Electric-field distribution

3.1.1. Electric-field models

To start with the calculation of the electric field, Maxwell's equations were used by combining Faraday's law of induction, and Ampère's law

$$\boldsymbol{\nabla} \times \boldsymbol{E} = -j\omega\mu_r\mu_0\boldsymbol{H} \qquad\qquad \text{A3.1}$$

and

$$\boldsymbol{\nabla} \times \boldsymbol{H} = \boldsymbol{J} + j\omega\varepsilon_r\varepsilon_0\boldsymbol{E} + \boldsymbol{J_e} \qquad\qquad \text{A3.2}$$

where $\boldsymbol{\nabla} \times$ [m^{-1}] is the curl, $\boldsymbol{E}$ [V·m^{-1}] is the electric field, ω [rad·s^{-1}] is the angular frequency, μ_r is the dimensionless relative permeability, μ_0 [H·m^{-1}] is the permeability of free space, $\boldsymbol{H}$ [A·m^{-1}] is the magnetic field, $\boldsymbol{J}$ [A·m^{-2}] is the electric-current density, ε_r is the dimensionless relative permittivity, ε_0 [F·m^{-1}] is the permittivity of free space, and $\boldsymbol{J_e}$ [A·m^{-2}] is the externally generated electric-current density. Again, the vector quantities are expressed in bold and italic. According to Ohm's law

$$\boldsymbol{J} = \sigma\boldsymbol{E} \qquad\qquad \text{A3.3}$$

where σ [S·m^{-1}] is the electrical conductivity. Since the energy density of the electric field is much larger than the energy density of the magnetic field, the electro-quasi-static approximation can be applied [103]. This approximation results in the neglect of the magnetic field, transforming Eq. A3.1 into

$$\boldsymbol{\nabla} \times \boldsymbol{E} = 0 \qquad\qquad \text{A3.4}$$

and allowing the electric-field component to be expressed as

$$\boldsymbol{E} = -\boldsymbol{\nabla}\Phi \qquad\qquad \text{A3.5}$$

with $\boldsymbol{\nabla}$ [m^{-1}] as gradient applied to the scalar electric potential Φ [V] [26, 43, 68, 72, 74, 79, 80]. Combination of Eq. A3.2, A3.3 and A3.5 results in

$$\boldsymbol{\nabla} \times \boldsymbol{H} = -\sigma\boldsymbol{\nabla}\Phi - j\omega\varepsilon_r\varepsilon_0\boldsymbol{\nabla}\Phi + \boldsymbol{J_e} \qquad\qquad \text{A3.6}$$

Since the magnetic field is neglected, we can apply the divergence to Eq. A3.6 to obtain

$$\boldsymbol{\nabla} \cdot (\boldsymbol{\nabla} \times \boldsymbol{H}) = -\boldsymbol{\nabla} \cdot (\sigma\boldsymbol{\nabla}\Phi) - \boldsymbol{\nabla} \cdot (j\omega\varepsilon_r\varepsilon_0\boldsymbol{\nabla}\Phi) + \boldsymbol{\nabla} \cdot \boldsymbol{J_e} \qquad\qquad \text{A3.7}$$

with $\boldsymbol{\nabla}\cdot$ [m^{-1}] as the divergence applied to the vector field. Because of the absence of the electric-current source to generate $\boldsymbol{J_e}$, and because $\boldsymbol{\nabla}\cdot(\boldsymbol{\nabla}\times\boldsymbol{H})=0$, we can simplify Eq. A3.7 into the continuity equation that describes the conservation of the electrical charge

$$-\boldsymbol{\nabla}\cdot\big((\sigma+\mathrm{j}\omega\varepsilon_r\varepsilon_0)\boldsymbol{\nabla}\Phi\big)=0 \qquad\qquad \text{A3.8}$$

in the frequency domain, or

$$-\boldsymbol{\nabla}\cdot(\sigma\boldsymbol{\nabla}\Phi)-\frac{\partial\mathrm{q}}{\partial\mathrm{t}}=0 \qquad\qquad \text{A3.9}$$

in time domain with

$$\mathrm{q}=\boldsymbol{\nabla}\cdot(\varepsilon_r\varepsilon_0\boldsymbol{\nabla}\Phi) \qquad\qquad \text{A3.10}$$

where q [C·m^{-3}] is the charge density [28, 73, 74]. In case of IRE the pulse duration is considered sufficient long to simplify Eq. A3.8 into a steady-state form [3, 24, 26, 27, 29, 31, 33, 34, 36-48, 50-59, 62, 63, 65, 66, 68-70, 75, 78-80],

$$\boldsymbol{\nabla}\cdot(\sigma\boldsymbol{\nabla}\Phi)=0 \qquad\qquad \text{A3.11}$$

3.1.2. Boundary conditions

For the calculation of the electric-potential distribution, Dirichlet, Neumann and Robin boundary conditions were applied in the included studies. In case of the Dirichlet boundary condition, the electric-potential values at the BOS and BEM were assumed to be fixed [3, 24, 26-29, 31-48, 50-55, 57-61, 64-66, 68-76, 78-80]. For example,

$$\Phi_{\mathrm{BEM}}\in\{V_P,0\} \qquad\qquad \text{A3.12}$$

in case one of the electrodes is active and the other one is grounded, or

$$\Phi_{\mathrm{BEM}}\in\left\{-\frac{V_P}{2},\frac{V_P}{2}\right\} \qquad\qquad \text{A3.13}$$

in case both of the electrodes are active. For Neumann boundary conditions, BC at BOS was assumed to be electric insulative, such that

$$-\boldsymbol{n}\cdot\boldsymbol{J}=0 \qquad\qquad \text{A3.14}$$

where $\boldsymbol{n}$ [m] is the normal vector perpendicular to the electrode surface or to the outer surface of the model [3, 24, 26, 28, 29, 31-34, 36-45, 48, 53, 57-61, 66, 69, 70, 73-75, 78-80]. This equation is equivalent to

$$\boldsymbol{n}\cdot(\sigma\boldsymbol{\nabla}\Phi)=0 \qquad\qquad \text{A3.15}$$

and can further simplified into

$$\sigma\frac{\partial\Phi}{\partial\mathrm{n}}=0 \qquad\qquad \text{A3.16}$$

with n [m] as the magnitude of $\boldsymbol{n}$. In contrast to the BC at BEM, a Neumann boundary condition was generally applied to the BOS and therefore Eq. A3.15 was applied to the outer surface of the model. Otherwise, they were assumed to be grounded [47, 51, 52, 55, 72, 75]

$$\Phi_{\text{BOS}} = 0 \text{ V} \qquad \text{A3.17}$$

In the remaining parts of the model the continuity boundary condition was applied,

$$\boldsymbol{n} \cdot (\boldsymbol{J_1} - \boldsymbol{J_2}) = 0 \qquad \text{A3.18}$$

where $\boldsymbol{n}$ is the normal vector, perpendicular to the surface of interest, J_1 [A·m^{-2}] is the current density in medium 1 and J_2 [A·m^{-2}] is the current density in medium 2.

3.1.3. Non-dimensional representation

A non-dimensional representation could be used to simplify the differential equation by removing the variability due to the size and reducing the number of parameters, and therefore, to focus on the physics of the process [104]. According to [47, 55, 75] Eq. A3.11 can be dimensionless such that

$$\underline{\boldsymbol{\nabla}} \cdot (\underline{\sigma} \cdot \underline{\boldsymbol{\nabla}}\underline{\Phi}) = 0 \qquad \text{A3.19}$$

with

$$\underline{\sigma} = \frac{\sigma}{\sigma_t} \qquad \text{A3.20}$$

$$\underline{\Phi} = \frac{\Phi}{(V_P/2)} \qquad \text{A3.21}$$

where $\underline{\boldsymbol{\nabla}}\cdot$ is dimensionless divergence, $\underline{\boldsymbol{\nabla}}$ is dimensionless gradient, $\underline{\sigma}$ is dimensionless electrical conductivity, σ_t [S·m^{-1}] is the electrical conductivity of target volume, and $\underline{\Phi}$ is the dimensionless scalar electrical potential. For example, assuming $\underline{\boldsymbol{\nabla}}$ depends on Cartesian coordinate system, it can be described as,

$$\underline{\boldsymbol{\nabla}} = \frac{\partial}{\partial \underline{x}}\boldsymbol{u_x} + \frac{\partial}{\partial \underline{y}}\boldsymbol{u_y} + \frac{\partial}{\partial \underline{z}}\boldsymbol{u_z} \qquad \text{A3.22}$$

with

$$\underline{x} = \frac{x}{\emptyset} \qquad \text{A3.23}$$

where $\underline{x}$ is dimensionless distance and $\emptyset$ is the diameter of a cylinder electrode. Here, $\emptyset$ was used as an example. Instead, it is also possible to use d (distance between the electrodes) [27]. Assuming Eq. A3.13 and A3.17 were applied as the Dirichlet boundary conditions, the BEM and the BOS were defined as:

$$\underline{\Phi_{\text{BEM}}} \in \{-1,1\} \qquad \text{A3.24}$$

and

$$\underline{\Phi_{BOS}} = 0 \qquad\qquad\qquad \text{A3.25}$$

3.2. Temperature distribution

3.2.1. Pennes bioheat transfer equation

The calculation of thermal distributions was mostly done using the Pennes Bioheat equation

$$\rho c_p \frac{\partial T}{\partial t} = \boldsymbol{\nabla}(k \cdot \boldsymbol{\nabla}T) - \rho_b \omega_b c_b (T - T_{art}) + Q_m + \boldsymbol{J} \cdot \boldsymbol{E} \qquad \text{A3.26}$$

where ρ [kg·m^{-3}] is the mass density, c_p [J·kg^{-1}·°C^{-1}] is the specific heat capacity, T [°C] is the temperature, t [s] is the time, k [W·m^{-1}·°C^{-1}] is the thermal conductivity, c_b [J·kg^{-1}·°C^{-1}] is the specific heat capacity of the blood, ρ_b [kg·m^{-3}] is the blood density, ω_b [s^{-1}] is the blood perfusion rate, and T_{art} [°C] is the arterial blood temperature, Q_m [W·m^{-3}] is the metabolic heat generation, and $\boldsymbol{J}$ ·$\boldsymbol{E}$ [W·m^{-3}] is the heat generation rate per unit volume, or the Joule Heating [3, 24, 26-29, 31, 33, 34, 36, 37, 39, 41-44, 48, 53, 55, 58, 61, 62, 66, 70, 73, 76, 80]. The Pennes Bioheat model was intended for the calculation of temperature distribution in solid materials, extending the model with metabolic heat generation Q_m and heat sink term $\rho_b \omega_b c_b (T - T_{art})$ to describe convection. Considering an elementary small tissue volume, the blood was assumed to enter the capillaries in this volume at temperature equals the arterial blood temperature T_{art}, after which the blood temperature instantaneously equilibrate with the temperature of the surrounding tissue. Subsequently, the blood leaves the capillaries at temperature T into the venous system.
Over the intrapulses, the Joule Heating term was described as

$$\boldsymbol{J} \cdot \boldsymbol{E} = (\sigma + j\omega\varepsilon_0\varepsilon_r)E^2 \qquad\qquad \text{A3.27}$$

This equation could be simplified into

$$\boldsymbol{J} \cdot \boldsymbol{E} = \sigma E^2 \qquad\qquad\qquad \text{A3.28}$$

since the pulse duration in IRE is considered sufficient long [3, 24, 26-28, 31, 33, 34, 39-41, 105]. However, the application of Eq. A3.28 over the intrapulse only requires more complex time-stepping algorithms [43, 45], which can increase the calculation costs. Therefore, the heating can be averaged over the entire intra- and interpulse duration [40, 43, 61, 62, 66, 70, 73, 80], by scaling the Joule heating to

$$\boldsymbol{J} \cdot \boldsymbol{E} = \sigma E^2 t_P f_P \qquad\qquad\qquad \text{A3.29}$$

3.2.2. Simplification of blood perfusion term

If software packages cannot handle the blood perfusion term in Eq. A3.26, then according to [26] the temperature variable can be substituted to obtain

$$T - T_{art} = Xe^{\frac{-w_b c_b t}{\rho c_p}} \qquad\qquad\qquad \text{A3.30}$$

resulting in

$$\rho c_p \frac{\partial \left(X e^{\frac{-w_b c_b t}{\rho c_p}} \right)}{\partial t} = \boldsymbol{\nabla} \left(k \cdot \boldsymbol{\nabla} \left(X e^{\frac{-w_b c_b t}{\rho c_p}} \right) \right) - w_b c_b X e^{\frac{-w_b c_b t}{\rho c_p}} + Q_m + \boldsymbol{J} \cdot \boldsymbol{E} \qquad \text{A3.31}$$

with w_b [kg·m⁻³·s⁻¹] as the blood perfusion, where

$$w_b = \rho_b \omega_b \qquad \text{A3.32}$$

Assuming a homogeneous, linear and isotropic tissue, we can simplify Eq. A3.31 into

$$\rho c_p \frac{\partial X}{dt} = \boldsymbol{\nabla}(k \cdot \boldsymbol{\nabla} X) + (Q_m + \boldsymbol{J} \cdot \boldsymbol{E}) e^{\frac{w_b c_b t}{\rho c_p}} \qquad \text{A3.33}$$

3.2.3. Non-dimensional Pennes bioheat transfer equation

When Q_m is negligible and the domain of interest is approximately homogeneous and

$$c_b = c_p \qquad \text{A3.34}$$

the Pennes bioheat equation can be dimensionless [27, 55]. The Joule heating term can be dimensionless by normalizing the electric field with the pulse voltage-to-distance ratio

$$\underline{P} = \frac{1}{\sigma_{init}(V_P/d)^2} \sigma_{init} E^2 \qquad \text{A3.35}$$

where $\underline{P}$ is the dimensionless Joule heating term, σ_{init} [S·m⁻¹] is the electric conductivity of the tissue before electroporation, and d [m] is the center-to-center distance between the electrodes in case of cylindrical or spherical electrodes. In case of plate electrodes d is the distance between the electrodes. The temperature, the coordinate space (assuming the use of Cartesian coordinate system) and time are dimensionless by

$$\underline{T} = \frac{k}{d^2 \sigma_{init}(V_P/d)^2} T \qquad \text{A3.36}$$

$$\underline{x} = \frac{1}{d} x \qquad \text{A3.37}$$

$$\underline{t} = \frac{k}{\rho c_p d^2} t \qquad \text{A3.38}$$

where $\underline{T}$ is dimensionless temperature, $\underline{x}$ is dimensionless distance, and $\underline{t}$ is dimensionless time. After combining Eq. A3.26 with A3.34-A3.38, we obtain

$$\frac{\partial \underline{T}}{\partial \underline{t}} = \underline{\boldsymbol{\nabla}}^2 \underline{T} - \rho_b \omega_b c_p \frac{d^2}{k} \underline{T} + \underline{P} \qquad \text{A3.39}$$

with $\underline{\boldsymbol{\nabla}}^2$ as dimensionless Laplace operator. For example, assuming $\underline{\boldsymbol{\nabla}}^2$ depends on Cartesian coordinate system, it can be described as,

$$\underline{\pmb{\nabla}}^2 = \frac{\partial^2}{\partial \underline{x}^2} + \frac{\partial^2}{\partial \underline{y}^2} + \frac{\partial^2}{\partial \underline{z}^2} \qquad\qquad \text{A3.40}$$

3.2.4. Analytical calculation of heat transfer equation

While Pennes Bioheat equation was used in almost all of the included studies, the blood perfusion and the metabolic heat generation were sometimes neglected [33, 41, 43, 106]. When both are neglected and in case of short t_P, we can simplify Eq. A3.26 into

$$\Delta T = \frac{\pmb{J} \cdot \pmb{E}}{\rho c_p} t_P \qquad\qquad \text{A3.41}$$

with ΔT [°C] as the temperature increase [26, 42]. In case of $t \gg t_P$ in a 2D homogeneous model, the heat transfer equation can be analytically calculated [64], resulting in

$$\frac{\partial T}{\partial t} = \alpha \pmb{\nabla}^2 T + \frac{\sigma E^2}{\rho c_p} \qquad\qquad \text{A3.42}$$

where α [m^2·s^{-1}] is the thermal diffusivity. This equation can be used to estimate the temperature distribution between two cylindrical electrodes in a 2D model. According to van Gemert et al [64], this can be done using a Gaussian radial function in the cylindrical coordinate system

$$\Delta T(r, t_p) = T_{fit} \exp\left(-\left(\frac{r}{r_{fit}}\right)^2\right) \qquad\qquad \text{A3.43}$$

with r [m] as radial coordinate, and T_{fit} [°C] and r_{fit} [m] are variables that were fitted to the measured temperature distribution in Figure 3B of [27], and ΔT [°C] is the obtained temperature increase at the end of t_P. The Gaussian function in Eq. A3.43 can be considered as cooling in the radial direction of a heat source line during time period of

$$\tau = \frac{r_{fit}^2}{4\alpha} \qquad\qquad \text{A3.44}$$

where τ [s] is the time constant for heat conduction. For an IRE pulse Eq. A3.42 was analytically solved to

$$\Delta T(r, t) \approx T_{fit} \frac{\exp\left(-\left(\frac{r}{r_{fit}}\right)^2 \Big/ \left(1 + \frac{t}{\tau}\right)\right)}{1 + \frac{t}{\tau}} \qquad\qquad \text{A3.45}$$

Since $\Delta T(r,t)$ is linear, the authors added the responses to multiple pulses to obtain

$$\Delta T\left(r, \frac{N_P - 1}{f_P}\right) \approx \Delta T_{fit} \sum_{n_P=0}^{N_P-1} \frac{\exp\left(-\left(\frac{r}{r_{fit}}\right)^2 \Big/ \left(1 + \frac{n_P}{f_P\tau}\right)\right)}{1 + \frac{n_P}{f_P\tau}} \frac{\sigma_{N_P-n_P}}{\sigma_{init}} \qquad\qquad \text{A3.46}$$

where f_P is pulse rate, and $\sigma(N_P - n_P)$ is the conductivity at the pulse n_P. Here, the ratio between $\sigma(N_P - n_P)$ and σ_{init} was obtained by fitting the conductivity increase in [107].

In case of a blood vessel parallel and in between a cylindrical electrode pair (see Figure A3.1), assuming that the blood flow removes the heat by keeping the intima at 37 °C, if the cooling of the vessel wall is approximated by 1D diffusion in x-direction (intima at x = 0m), then we can describe ΔT for a single pulse as

$$\Delta T(x,t) \approx T_{fit}\, erf\left(\frac{x}{\sqrt{4\alpha t}}\right) \qquad\qquad \text{A3.47}$$

For multiple pulses, we can describe ΔT as

$$\Delta T\left(x, \frac{N_P - 1}{f_P}\right) \approx T_{fit} \sum_{n_P=0}^{N_P-1} erf\left(\frac{x}{\sqrt{\frac{4\alpha n_P}{f}}}\right) \frac{\sigma_{N_P-n_P}}{\sigma_{init}} \qquad\qquad \text{A3.48}$$
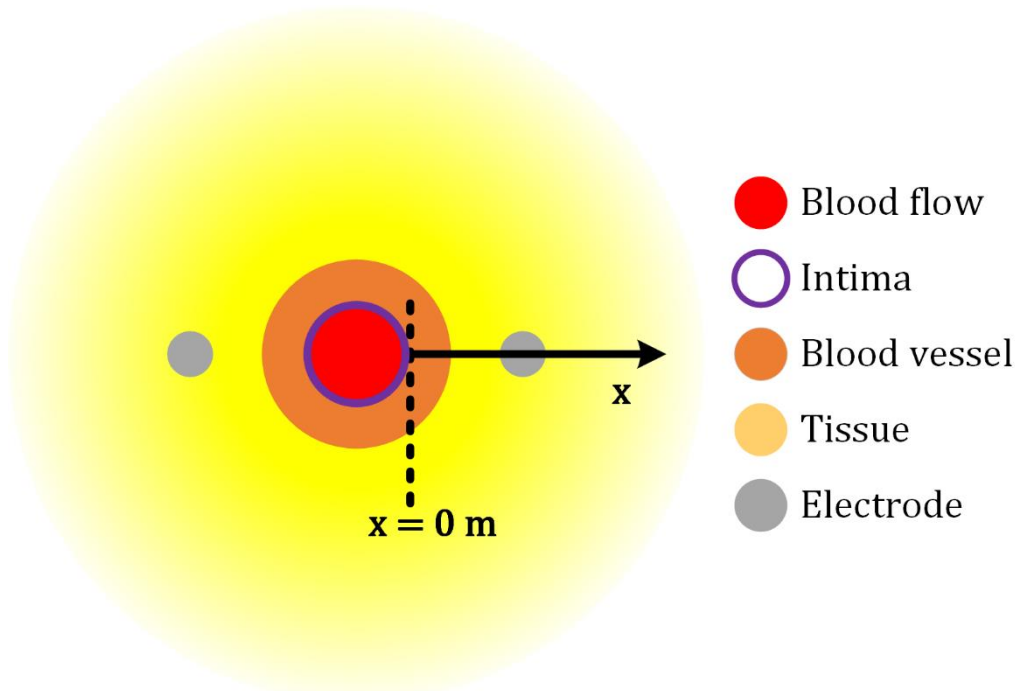
Figure A3.1 2D view of IRE simulation including a vessel wall in between the needle pair.

3.2.5. Temperature distribution between rectangular electrodes

In case of a finite slab between two rectangular electrodes (a slab can be a piece of a tissue or cell suspension), it is possible to describe the temperature distribution for a single pulse in which the electrodes serve as infinite fins that dissipate the heat from the slab [30]. See Figure A3.2.
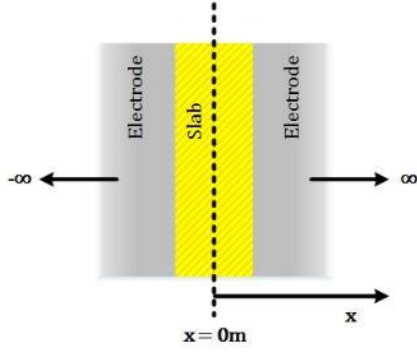
Figure A3.2 A finite slab in between two rectangular electrodes that act as infinite fins. The infinity symbols means that the thickness of the electrodes is infinitely extended.

The heat transfer solution that describes this transient conduction is

$$\frac{T - T_{env}}{T_{max} - T_{env}} = \sum_{n\#=1}^{\infty} C_{n\#} \exp\left(-\frac{\beta_{n\#}^2 \alpha t}{\Gamma^2}\right) \cos\left(\frac{\beta_{n\#} x}{\Gamma}\right) \qquad \text{A3.49}$$

where T_{max} [°C] is the maximum temperature after application of IRE for the pulse duration t_P, T_{env} [°C] is the temperature of the environment, Γ [m] is the half thickness of the slab, x [m] is the distance from the centerline of the slab, the dimensionless $C_{n\#}$ equals

$$C_{n\#} = \frac{4 \sin(\beta_{n\#})}{2\beta_{n\#} + \sin(2\beta_{n\#})} \qquad \text{A3.50}$$

and the dimensionless constants $\beta_{n\#}$ are calculated from

$$\beta_{n\#} \tan(\beta_{n\#}) = \frac{h_{eq}\Gamma}{k} \qquad \text{A3.51}$$

where h_{eq} [W·m^{-2}·°C^{-1}] is the equivalent heat transfer coefficient assuming that the stainless steel electrodes act as infinite fins in free convection. Assuming a homogeneous temperature distribution in the slab equals the temperature at the centerline of the slab (x = 0 m), and assuming the first term (n# = 1) of the Fourier series, we can simplify Eq. A3.49 into

$$\frac{T - T_{env}}{T_{max} - T_{env}} = C_1 \exp\left(-\frac{\beta_1^2 \alpha t}{\Gamma^2}\right) \qquad \text{A3.52}$$

The temperature rise due to the Joule heating of the slab for parallel plate electrode configuration can be calculated according to Eq. A3.41 as

$$T_{max} - T_{env} = \frac{\sigma E^2}{\rho c_p} t_P \qquad \text{A3.53}$$

resulting in

$$T = \frac{\sigma E^2}{\rho c_p} t_P C_1 \exp\left(-\frac{\beta_1^2 \alpha t}{\Gamma^2}\right) + T_{env} \qquad \text{A3.54}$$

3.2.6. Boundary conditions

Similar to the calculation of the electric potential distribution, for the temperature distribution the boundary condition at the BEM and BOS are important. In the included studies, Dirichlet, Neumann, and Robin boundary conditions were used. The Dirichlet boundary condition was applied when the temperatures were assumed to be e.g. 37 °C at the electrode-medium interface (T_{BEM} [°C]) [28], and/or at the outer surface of the model (T_{BOS} [°C]) [28, 33, 34, 36, 41, 53, 55]. If the boundaries were assumed to be adiabatic (thermal insulative) at the electrode-medium interface [3, 24, 26, 27, 39, 73], and/or at the outer surface of the model [3, 24, 26, 27, 29, 31, 39, 40, 43, 58, 61, 73, 80], then the Neumann boundary conditions were applied, such that

$$-\boldsymbol{n} \cdot (k\boldsymbol{\nabla}T) = 0 \qquad \text{A3.55}$$

This equation can be simplified to

$$\frac{\partial T}{\partial n} = 0 \qquad \text{A3.56}$$

In case of the Robin boundary condition, the authors assumed that their model exchanged heat by convection at the electrode-medium interface [29, 30, 40, 59], and/or at the outer surface of the model [25, 37, 43-45, 59], such that

$$-\boldsymbol{n} \cdot (k\boldsymbol{\nabla}T) = h(T - T_{env}) \qquad \text{A3.57}$$

where h [W·m^{-2}·°C^{-1}] is the heat transfer coefficient, and T_{env} [°C] is the temperature of the environment. Mandel et al. [44] for example furtherly expanded Eq. A3.57 for the eye model to consider tear evaporation and the radiation. This was done by adding the new terms

$$-\boldsymbol{n} \cdot (k\boldsymbol{\nabla}T) = h(T - T_{env}) + q_e + \varepsilon a(T^4 - T_{env}^4) \qquad \text{A3.58}$$

where q_e [W·m^{-2}] is the evaporation rate, a [W·m^{-2}·°C^{-4}] is the Stefan-Boltzmann constant, and ε_s is the dimensionless emissivity of the corneal surface (transparent front part of the eye).
In the remaining parts of the model the continuity boundary condition was applied,

$$\boldsymbol{n} \cdot (k_1\boldsymbol{\nabla}T_1 - k_2\boldsymbol{\nabla}T_2) = 0 \qquad \text{A3.59}$$

where $k_1\boldsymbol{\nabla}T_1$ [W·m^{-2}] is the heat flux in medium 1 and $k_2\boldsymbol{\nabla}T_2$ [W·m^{-2}] is the heat flux in medium 2.

3.3. Tissue properties

To give an overview of the applied models, we summarize in this section the non-linear properties used to model the electrical and thermal conductivities.

3.3.1. Dependence on electric field

First of all, the author in [77] simply modeled the dependence of the electrical conductivity on the electric field, $\sigma(E)$, as

$$\sigma(E) = \sigma_{init} + (\sigma_{max} - \sigma_{init})\mathbb{1}(E - E_{IRE(th)}) \qquad \text{A3.60}$$

with σ_{max} [S·m^{-1}] as the electrical conductivity of the maximally permeabilized tissue, and $\mathbb{1}(E - E_{IRE(th)})$ as the unit function, where

$$\mathbb{1}\left(E - E_{IRE(th)}\right) = \begin{cases} 0, & E < E_{IRE(th)} \\ 1, & E \geq E_{IRE(th)} \end{cases} \qquad \text{A3.61}$$

Similarly, the authors in [42, 63] assumed $\sigma(E)$ to have linear dependence, such that

$$\sigma(E) = \frac{\sigma_{max} - \sigma_{init}}{E_{IRE(th)} - E_{RE(th)}} E + \sigma_{init} \qquad \text{A3.62}$$

where $E_{RE(th)}$ [V·m^{-1}] is the threshold of the reversible electroporation in the tissue. Further increase of the complexity of the electrical conductivity was done by fitting $\sigma(E)$ into a sigmoid functions [45, 53, 56, 57, 59, 63, 70, 71, 78]. For example, according to the authors in [53, 71], $\sigma(E)$ could be fitted in the form

$$\sigma(E) = \sigma_{init} + (\sigma_{max} - \sigma_{init}) \frac{1}{1 + a_1 \exp\left(-\dfrac{E - a_2}{a_3}\right)} \qquad \text{A3.63}$$

with

$$a_2 = \frac{E_{IRE(th)} + E_{RE(th)}}{2} \qquad \text{A3.64}$$

and

$$a_3 = \frac{E_{IRE(th)} - E_{RE(th)}}{a_4} \qquad \text{A3.65}$$

where a_1 and a_4 are the sigmoid function parameters. Next, to further increase the complexity, $\sigma(E)$ can be fitted into

$$\sigma(E) = \sigma_{init} + (\sigma_{max} - \sigma_{init}) \exp\left(-a_5 \exp\left(a_6(E - a_7)\right)\right) \qquad \text{A3.66}$$

where a_5, a_6, and a_7 are the sigmoid function parameters [45, 56, 57, 63, 70, 78]. Finally, it is possible to express $\sigma(E)$ as hyperbolic function such that

$$\sigma(E) = \sigma_{init}\left(1 + a_8\left(1 + \tanh\left(\frac{E - E_{RE(th)}}{E_{RE(th)}}\right)\right)\right) \qquad \text{A3.67}$$

with a_8 as a dimensionless parameter [79].

3.3.2. Dependence on temperature

Besides the dependence of the electrical conductivity on the electric field, other authors in [40, 43, 45, 60] assumed the linear dependence on temperature,

$$\sigma(T) = \sigma_{init}\left(1 + \xi(T - T_{init})\right) \qquad \text{A3.68}$$

where ξ [$°C^{-1}$] (with unit often written as [%·$°C^{-1}$]) is the increase of conductivity per 1°C.

Dependence on Electric Field and Temperature

The electrical conductivity can also be presented as function both electric-field strength and temperature, $\sigma(E, T)$, [31, 37, 40, 45, 73, 76, 80]. Examples of applied $\sigma(E, T)$ are

$$\sigma(E, T) = \left(\sigma_{init} + (\sigma_{max} - \sigma_{init})\exp\left(-a_5\exp\left(-a_6(E - a_7)\right)\right)\right) \cdot \left(1 + \xi(T - T_{init})\right) \tag{A3.69}$$

which was applied in [45],

$$\sigma(E, T) = \left(\sigma_{init} + (\sigma_{max} - \sigma_{init})\frac{1}{1 + a_1\exp\left(-\dfrac{E - a_2}{a_3}\right)}\right) \cdot \left(1 + \xi(T - T_{init})\right) \tag{A3.70}$$

which was applied in [80], and

$$\sigma(E, T) = \left(\sigma_{init} + (\sigma_{max} - \sigma_{init})\frac{1}{1 + a_1\exp\left(-\dfrac{E - a_2}{a_3}\right)}\right) \cdot \left(a_8^{T - T_{init}}\right) \tag{A3.71}$$

which was applied in [76].

3.3.3. Other types

Furthermore, electrical conductivity can be depended on pulse number [64], time [46, 78], and directions [35, 59]. An example of $\sigma(n_P)$ was shown in Eq. A3.46. In case of the use of anisotropic tissue properties, such as muscle in which the longitudinal electrical conductivity differs from the transversal one [35, 59], the electrical conductivity turns into a tensor (boldly expressed without use of italic) with the general form

$$\boldsymbol{\sigma} = \begin{bmatrix} \sigma_{xx} & \sigma_{xy} & \sigma_{xz} \\ \sigma_{yx} & \sigma_{yy} & \sigma_{yz} \\ \sigma_{zx} & \sigma_{zy} & \sigma_{zz} \end{bmatrix} \tag{A3.72}$$

If certain conditions are met that allow the electrical conductivity to be written with respect to the oriented local coordinate system, we can simplify Eq. A3.72 to

$$\boldsymbol{\sigma} = \begin{bmatrix} \sigma_{xx} & 0 & 0 \\ 0 & \sigma_{yy} & 0 \\ 0 & 0 & \sigma_{zz} \end{bmatrix} \tag{A3.73}$$

O'Brien TJ, Arena CB, Davalos RV. Thermal considerations with tissue electroporation. In: Handbook of thermal science and engineering. Cham: Springer International Publishing, 2018. pp. 2489–2519.

Foster KR, Lozano-Nieto A, Riu PJ, et al. Heating of tissues by microwaves: a model analysis. Bioelectromagnetics. 1998;19(7): 420–428.

Arena CB, Mahajan RL, Rylander MN, et al. Towards the development of latent heat storage electrodes for electroporation-based therapies. Appl Phys Lett. 2012;101(8):083902.

Arena CB, Sano MB, Rossmeisl JH, et al. High-frequency irreversible electroporation (H-FIRE) for non-thermal ablation without muscle contraction. BioMed Eng OnLine. 2011;10(1):102.

Ivorra A, Al-Sakere B, Rubinsky B, et al. In vivo electrical conductivity measurements during and after tumor electroporation: conductivity changes reflect the treatment outcome. Phys Med Biol. 2009;54(19):5949–5963.

Appendix 4 - Additional clarification of figures

In this section an extended version of Figure 8 and 9 were presented for proper clarification of the data points.
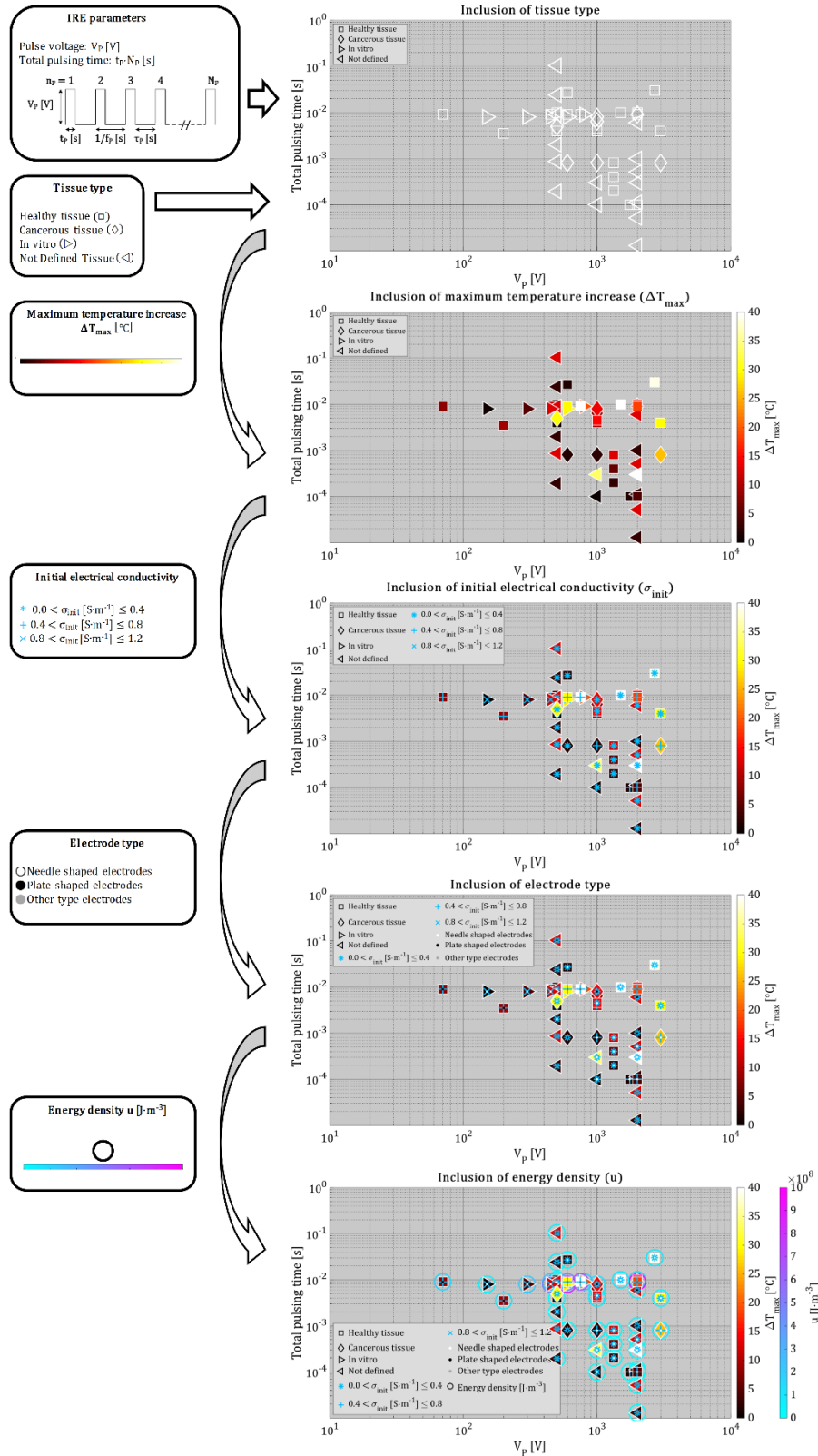

Figure A4.1 An extended version of Figure 8A to clarify the presented data points.
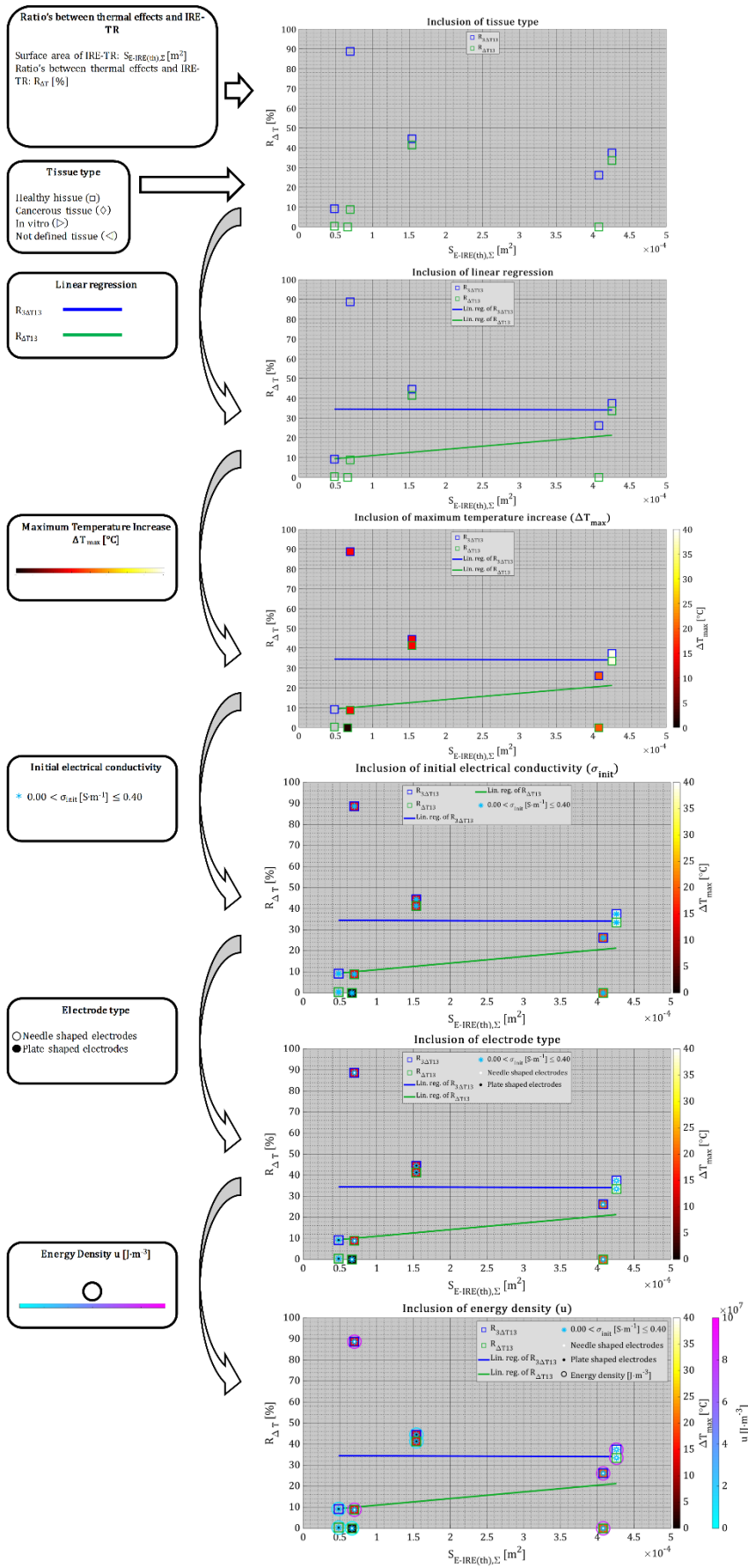
Figure A4.2 An extended version of Figure 9 to clarify the presented data points.

Appendix 5 - Extended mathematical description applied to methods of analysis

To determine the $k\#^{th}$ $S_{E\text{-}IRE(th)}$, we determined the total surface area of the electrodes ($S_{elect,\Sigma \mid k\#}$ [m²]) within the $k\#^{th}$ $S_{E\text{-}IRE(th)}$ using

$$S_{elect,\Sigma \mid k\#} = \sum_{n\#=1}^{N\#} S_{elect \mid k\#,n\#} \qquad\qquad A5.1$$

where $S_{elect \mid k\#,n\#}$ [m²] is the surface area of the $n\#^{th}$ electrode within the $k\#^{th}$ $S_{E\text{-}IRE(th)}$. The $k\#^{th}$ $S_{E\text{-}IRE(th)}$ was then determined using the condition

$$S_{E\text{-}IRE(th) \mid k\#} \in \left\{ \left(S_{E \mid k\#} - S_{elect,\Sigma \mid k\#} \in \mathbb{R} \right) \,\middle|\, E \geq E_{IRE(th)} \right\} \qquad\qquad A5.2$$

where $S_{E \mid k\#}$ is the surface area of the $k\#^{th}$ IRE-TR including the total surface area of the electrodes. The extraction of temperature distributions satisfied the conditions

$$S_{3\Delta T13 \mid l\#} \in \left\{ \left(S_{\Delta T \mid l\#} - S_{elect,\Sigma \mid l\#} \right) \in \mathbb{R} \,\middle|\, 3 \leq \Delta T\,[°C] < 13 \right\} \qquad\qquad A5.3$$

and

$$S_{\Delta T13 \mid m\#} \in \left\{ \left(S_{\Delta T \mid m\#} - S_{elect,\Sigma \mid m\#} \right) \in \mathbb{R} \,\middle|\, \Delta T\,[°C] \geq 13 \right\} \qquad\qquad A5.4$$

where $S_{\Delta T \mid m\#}$ and $S_{\Delta T \mid l\#}$ are the $m\#^{th}$ and the $l\#^{th}$ selected surface area of the temperature increase distribution. If the imported figure includes E- and ΔT-contours showing the conditions mentioned in Eq. A5.2, A5.3, and A5.4, then we manually selected S_E, $S_{\Delta T}$ and S_{elect} using the "Freehand selections" tool or "Polygon selections" tool. In case of no contours, we used the "Threshold Color" tool to set the threshold of the surface color to the minimum value mentioned in Eq. A5.2, A5.3, and A5.4. Finally, the ratios were calculated as

$$R_{3\Delta T13} = \sum_{k\#=1}^{K\#} \frac{\sum_{l\#=1}^{L\#} S_{3\Delta T13 \mid k\#,l\#}}{S_{E\text{-}IRE(th) \mid k\#}} 100\% \qquad\qquad A5.5$$

and

$$R_{\Delta T13} = \sum_{k\#=1}^{K\#} \frac{\sum_{m\#=1}^{M\#} S_{\Delta T13 \mid k\#,m\#}}{S_{E\text{-}IRE(th) \mid k\#}} 100\% \qquad\qquad A5.6$$